

Solution and solid–gas reactivity of unsaturated $[\text{RuCp}(\text{tmeda})]^+$ ($\text{tmeda} = \text{Me}_2\text{NC}_2\text{H}_4\text{NMe}_2$)

Christian Gemel^a, John C. Huffman^a, Kenneth G. Caulton^{a,*}, Klaus Mauthner^b,
Karl Kirchner^b

^a Department of Chemistry and Molecular Structure Center, Indiana University, Bloomington, IN 47405-7102, USA

^b Institute of Inorganic Chemistry, Vienna University of Technology, Getreidemarkt 9, A-1060 Vienna, Austria

Received 25 June 1999; accepted 20 September 1999

Dedicated to Fausto Calderazzo, whose work has taught much to all of us.

Abstract

The coordinatively unsaturated complex $[\text{RuCp}(\text{tmeda})]^+$ has been prepared by the reaction of $[\text{RuCp}(\text{tmeda})\text{Cl}]$ with NaBAR'_4 ($\text{Ar}' = 3,5\text{-C}_6\text{H}_3(\text{CF}_3)_2$) in fluorobenzene. The PF_6^- salt of $[\text{RuCp}(\text{tmeda})]^+$ is prepared by heating $[\text{RuCp}(\text{tmeda})(\text{CH}_3\text{CN})]\text{PF}_6$ at 150°C under reduced pressure (10^{-2} atm). The X-ray crystal structure of $[\text{RuCp}(\text{tmeda})]^+$ as the BAR'_4 salt has been determined showing the absence of any agostic interactions between ruthenium and the C–H bonds of the diamine ligand, and only minor deviations from the planar geometry at Ru. $[\text{RuCp}(\text{tmeda})]^+$ reacts readily with the gases H_2 , $\text{CH}_2=\text{CH}_2$, $\text{CHF}=\text{CH}_2$, $\text{HC}=\text{CH}$, CO , HCl , N_2 , and O_2 at low temperature to give $[\text{RuCp}(\text{tmeda})(\eta^2\text{-H}_2)]^+$, $[\text{RuCp}(\text{tmeda})(\eta^2\text{-CH}_2\text{-CH}_2)]^+$, $[\text{RuCp}(\text{tmeda})(\eta^2\text{-CHF}=\text{CH}_2)]^+$, $[\text{RuCp}(\text{tmeda})(\eta^2\text{-HC}=\text{CH})]^+$, $[\text{RuCp}(\text{tmeda})(\text{CO})]^+$, $[\text{RuCp}(\text{tmeda})(\text{H})(\text{Cl})]^+$, $[\text{RuCp}(\text{tmeda})(\text{N}_2)]^+$, and $[\text{RuCp}(\text{tmeda})(\text{O}_2)]^+$. The reactions of $[\text{RuCp}(\text{tmeda})][\text{BAR}'_4]$ with the above gases have also been carried out as solid–gas reactions. Treatment of $[\text{RuCp}(\text{tmeda})]^+$ with the terminal acetylenes $\text{HC}=\text{CR}$ ($\text{R} = \text{Bu}'$, SiMe_3) results in the formation of the vinylidene complexes $[\text{RuCp}(\text{tmeda})(=\text{C}=\text{CHR})]^+$. In the case of $\text{R} = \text{SiMe}_3$ upon treatment with HCl , the parent vinylidene complex $[\text{RuCp}(\text{tmeda})(=\text{C}=\text{CH}_2)]^+$ is formed. $[\text{RuCp}(\text{tmeda})(\eta^2\text{-HC}=\text{CH})]^+$ and $[\text{RuCp}(\text{tmeda})(=\text{C}=\text{CH}_2)]^+$ are not interconvertible for kinetic reasons. Furthermore, $[\text{RuCp}(\text{tmeda})]^+$ reacts slowly with both CH_2Cl_2 and CH_2Br_2 to give the carbene complex $[\text{RuCp}(\text{tmeda})(=\text{CH}_2)]^+$ involving double C–X bond activation. © 2000 Elsevier Science S.A. All rights reserved.

Keywords: Ruthenium; Amine ligands; Unsaturated; Solid–gas reactivity; Vinylidene

1. Introduction

Coordinatively unsaturated half-sandwich d^6 -complexes of iron, ruthenium, and osmium are extremely rare unless there is stabilization by bulky co-ligands and heteroatomic anionic ligands through metal ligand multiple bonds, e.g. alkoxides, thiolates, amides, or halides. While in the case of iron, two 16 e complexes lacking π -donor ligands have been reported, viz $[\text{FeCp}^*(\text{dippe})]^+$ and $[\text{FeCp}^*(\text{dppe})]^+$ [1,2] ($\text{dippe} = \text{}^i\text{Pr}_2\text{PC}_2\text{H}_4\text{P}^i\text{Pr}_2$; $\text{dppe} = \text{Ph}_2\text{PC}_2\text{H}_4\text{PPh}_2$), for ruthenium

and osmium such counterparts are virtually unknown. Compounds of the type $[\text{MCp}(\text{PP})]^+$ and $[\text{MCp}^*(\text{PP})]^+$ ($\text{M} = \text{Ru}, \text{Os}$; $\text{PP} =$ mono and bidentate tertiary phosphine) prepared in situ react readily with appropriate substrates to yield saturated complexes or, in the absence of potential ligands, react with themselves via dimerization as in the case of $\text{RuCp}^*(\text{acac})$ [3] or undergo an intramolecular oxidative addition as with $[\text{RuCp}^*(\text{Ph}_2\text{PCH}_2\text{CH}_2\text{NMe}_2)]^+$ [4]. An outstanding example for the high reactivity of such unsaturated complexes is the 16 e fragment $[\text{OsCp}^*(\text{dmpm})]^+$ ($\text{dmpm} = \text{bis}(\text{dimethylphosphino})\text{methane}$), which has been shown to reversibly bind CH_4 [5]. The authors claimed a σ -bound methane molecule as an intermediate for hydrogen scrambling of the hydride into the methyl group in $[\text{OsCp}^*(\text{dmpm})(\text{H})(\text{CH}_3)]^+$.

* Corresponding author. Tel.: +1-812-8554798; fax: +1-812-8558300.

E-mail address: caulton@indiana.edu (K.G. Caulton)

A noteworthy exception to the above is the remarkable stability of the cationic 16 e complex $[\text{RuCp}^*(\text{tmeda})]^+$ ($\text{tmeda} = \text{Me}_2\text{NC}_2\text{H}_4\text{NMe}_2$) and its derivatives devoid of a π -donor ligand [6]: there is no reaction with ethylene, $\text{Me}_3\text{SiC}\equiv\text{CH}$, H_2 , CH_3Br or Et_3SiH . Extended Hückel model calculations rationalize the extraordinary inertness of the planar 16 e $[\text{Cp}^*\text{Ru}(\text{NN})]^+$ structure in terms of a high planar/pyramidal rearrangement barrier and a large HOMO–LUMO gap deriving from through-bond coupling through the intervening σ skeleton of the chelating diamine (NN) ligand (in contrast to the PP and PN analogs) in addition to the high π -donor strength of Cp^* . Here we extend our studies on coordinatively unsaturated ruthenium complexes and report on the first 16 e RuCp complex $[\text{RuCp}(\text{tmeda})]^+$ including some reactivities both in solution and in the solid state. Our goal is to establish, by comparison, both the steric and electronic influence on reactivity caused by replacing Cp^* by Cp .

2. Results and discussion

2.1. Preparation of $[\text{RuCp}(\text{tmeda})(\text{CH}_3\text{CN})]\text{BAR}'_4$ (**1**) and $\text{RuCp}(\text{tmeda})\text{Cl}$ (**2**)

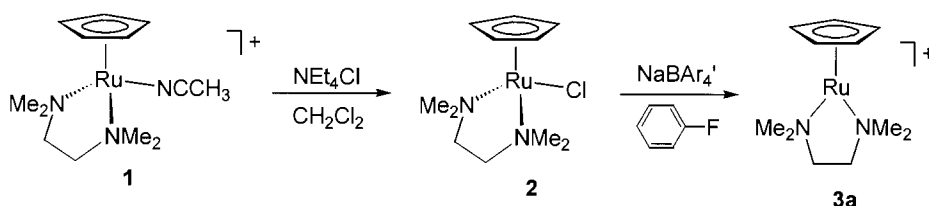
Treatment of $[\text{RuCp}(\text{CH}_3\text{CN})_3]\text{PF}_6$ with one equivalent of tmeda at room temperature (r.t.) affords the cationic complex $[\text{RuCp}(\text{tmeda})(\text{CH}_3\text{CN})]\text{PF}_6$ (**1**) in essentially quantitative yield as monitored by ^1H -NMR spectroscopy (Scheme 1). This compound is stable in air in the solid state but decomposes slowly in solutions of acetone, CH_3CN , and CH_3NO_2 on exposure to air. Characterization was by ^1H - and $^{13}\text{C}\{^1\text{H}\}$ -NMR and IR spectroscopies as well as elemental analysis. The CH_3CN ligand in **1** is substitutionally labile and is readily replaced by CD_3CN in a solution of CDCl_3 at r.t. The first-order rate constant at r.t. obtained by NMR line broadening is 167 s^{-1} (cf. 5.6 s^{-1} for $[\text{RuCp}(\text{CH}_3\text{CN})_3]\text{PF}_6$) [7]. The CH_3CN exchange appears to proceed via a dissociative mechanism since the reaction rate is independent of the free CH_3CN concentration. In view of the lability of the CH_3CN ligand, **1** is a suitable precursor for complexes containing the $[\text{RuCp}(\text{tmeda})]^+$ fragment. Thus, upon addition of

NEt_4Cl to a solution of **1** in CH_2Cl_2 the color immediately changes from yellow to orange, to yield, on workup, the neutral complex $\text{RuCp}(\text{tmeda})\text{Cl}$ (**2**) (Scheme 1). The ^1H -NMR spectrum of **2** exhibits no unusual features, except perhaps that the $\text{NCH}_2\text{CH}_2\text{N}$ hydrogen atoms give rise to only one singlet instead of the expected multiplet. In the presence of excess chloride, the two CH_3 signals of tmeda collapse to only one signal, due to a fast exchange process between free and coordinated chloride. A similar observation has been made for the analogous Cp^* complex $\text{RuCp}^*(\text{tmeda})\text{Cl}$ [8].

2.2. Preparation of $[\text{RuCp}(\text{tmeda})]\text{BAR}'_4$ (**3a**)

Halide abstraction from **2** with NaBAR'_4 ($\text{Ar} = 3,5\text{-C}_6\text{H}_3(\text{CF}_3)_2$) in fluorobenzene affords the novel dark cationic 16 e complex $[\text{RuCp}(\text{tmeda})]\text{BAR}'_4$ (**3a**), in 86% isolated yield, which is highly air-sensitive both in solution and in the solid state. Such an intense blue color is characteristic of a 16 e $\text{Ru}(\text{II})$ complex containing a 6 e spectator ligand such as Cp^* , arenes, or tridentate NNN, PCP, and NCN pincer-type ligands [9]. Characterization of **3a** was achieved by elemental analysis, and ^1H - and $^{13}\text{C}\{^1\text{H}\}$ -NMR spectroscopies. This complex is characterized by the presence of single resonances in the ^1H -NMR spectrum for the NMe_2 and $\text{NCH}_2\text{CH}_2\text{N}$ protons. The simplicity of the spectrum is indicative of a cationic complex that has C_{2v} symmetry. This is also supported by the $^{13}\text{C}\{^1\text{H}\}$ -NMR data and unequivocally confirmed by X-ray crystallography as shown in Fig. 1. According to our knowledge, **3a** is the first coordinatively unsaturated RuCp complex. Joslin and co-workers recently claimed the synthesis of the 16 e complex $[\text{RuCp}(\text{PCy}_2\text{CH}_2\text{CH}_2\text{PCy}_2)]\text{CF}_3\text{SO}_3$ based on NMR spectroscopic evidence and elemental analysis [10]. However, in view of the ability of CF_3SO_3^- to coordinate at $\text{Ru}(\text{II})$ [9d,11], as well as the orange color of the complex, we believe the formula should instead be $\text{RuCp}(\text{PCy}_2\text{CH}_2\text{CH}_2\text{PCy}_2)(\eta^1\text{-O-CF}_3\text{SO}_3)$.

On cooling a solution of **3a** in CD_2Cl_2 to -90°C , the color changes to pale yellow and the proton resonances of the tmeda ligand are broadened, indicating the formation of a new complex. This reaction is reversible since on warming to r.t., **3a** is recovered. Since neither the chemical shift (-51.6 ppm) nor the line shape of



Scheme 1.

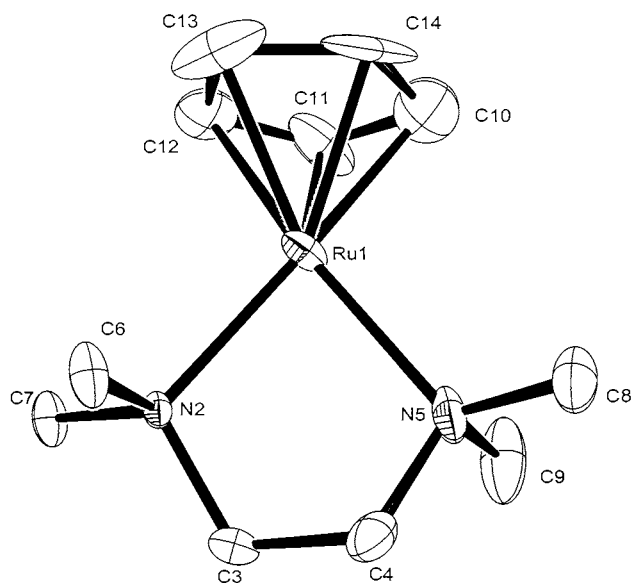


Fig. 1. Structural view of $[\text{RuCp}(\text{tmeda})]\text{BAR}_4^+$ (**3a**) showing 50% thermal ellipsoids (BAR_4^- omitted for clarity).

the $^{19}\text{F}\{^1\text{H}\}$ -NMR signal of the BAR_4^- ion is temperature-dependent, it is unlikely that BAR_4^- coordinates to ruthenium and it is reasonable to assume that **3a** forms a labile adduct with CD_2Cl_2 . In fact, transition metal complexes featuring CH_2Cl_2 as a ligand are known [12]. Furthermore, a metal solvent interaction is also supported by the finding that **3a** reacts slowly with CH_2Cl_2 at r.t. to yield a carbene complex involving C–Cl activation (vide infra).

The PF_6^- salt of $[\text{RuCp}(\text{tmeda})]^+$ has been prepared by treatment of **2** with TlPF_6 in THF leading first to the labile complex $[\text{RuCp}(\text{tmeda})(\text{THF})]\text{PF}_6$ which has not been isolated but, under reduced pressure, liberates THF easily even at r.t. to afford analytically pure $[\text{RuCp}(\text{tmeda})]\text{PF}_6$ (**3b**). Alternatively, **3b** can be prepared in a solid–gas reaction by heating **1** at 150°C under reduced pressure (10^{-2} atm) resulting in a color change from yellow to deep blue. The latter procedure, however, is limited to small amounts (< 100 mg).

The crystal structure of **3a** shows the unit cell composed of noninteracting cations and anions. The shortest intermolecular contacts of Ru–F are 4.4 Å. The cation (Fig. 1) is confirmed to contain only two donors, in addition to the Cp ligand, and Ru lies in the plane of the two N and the Cp ring midpoint. There is no indication of any agostic interactions between ruthenium and the C–H bonds of the diamine ligand. The Ru–N distances (2.15 Å) are fairly short for tertiary amines (cf. 2.181 Å for $[\text{RuCp}^*(\text{tmeda})]^+$), and the N–Ru–N angle is relatively small (80.8° , cf. 80.3° for $[\text{RuCp}^*(\text{tmeda})]^+$). The Ru(tmeda) ring is in the twist conformation, with the CH_2 carbons displaced to opposite sides of the N–Ru–N plane. This creates axial (C6 and C9) and equatorial (C7 and C8) methyl groups

which are related by an idealized C_2 axis bisecting the N–Ru–N angle. These crystals are not isomorphous with those of $[\text{RuCp}^*(\text{tmeda})][\text{BAR}_4^-]$.

2.3. Reaction of **3a** with some gases in solution

The solution of **3a** in CD_2Cl_2 reacts with a variety of gases according to Scheme 2. Addition of H_2 to **3a** at -90°C resulted in a green solution due to the formation of $[\text{RuCp}(\text{tmeda})(\eta^2\text{-H}_2)]^+$ (**4**). In the ^1H -NMR spectrum, the two hydrogens exhibit a characteristic broad resonance at -3.6 ppm pointing to a dihydrogen rather than a dihydride structure. This has been confirmed on the basis of a T_1 relaxation measurement at -90°C being 10.2 ms (400 MHz). The short T_1 value associated with **4** falls within the range of 10 to 160 ms generally accepted for nonclassical dihydrogen coordination [13]. Complex **4** is thermally not stable and at temperatures above -70°C apparently decomposition takes place to some paramagnetic species as indicated by several broad proton resonances in the range of 40 to -20 ppm. For comparison, the more electron-rich isoelectronic complex $[\text{RuCp}^*(\text{tmeda})]^+$ did not react with H_2 under the same reaction conditions [6]. Such a trend in the relative stability of dihydrogen complexes has also been found in $[\text{RuCp}(\text{PP})]^+$ and $[\text{RuCp}^*(\text{PP})]^+$ (PP = bisphosphines) chemistry [14]. In the case of the latter, dihydrogen adducts are detected only at low temperature. On the other hand, in a PP donor environment both RuCp and RuCp* complexes react with H_2 to give classical Ru(IV) dihydride complexes.

In a fashion similar to H_2 , also $\text{CH}_2=\text{CH}_2$, $\text{CHF}=\text{CH}_2$, $\text{HC}\equiv\text{CH}$, and CO react readily with **3a** at -60°C to give quantitatively complexes **5a**, **5b**, **6**, and **7** as monitored by ^1H -NMR spectroscopy. In the case of $\text{HC}\equiv\text{CH}$, $\text{CH}_2=\text{CH}_2$, and CO the low temperature ^1H -NMR spectra reveal the expected resonance pattern for a C_s symmetric molecule. The ethylene protons are equivalent due to fast rotation around the metal–ligand bond [15]. In the case of $\text{CHF}=\text{CH}_2$, which is asymmetric, the ^1H -NMR spectrum of **5b** shows four distinct singlets for the CH_3 groups and four multiplets for the methylene bridge, and it is not possible to establish if rotation around the metal–ligand bond occurs. Interestingly, on warming the solutions to r.t., the ^1H -NMR spectra of **5a**, **5b** and **6** simplify, indicating a fast exchange between free and bound ligands. In all cases, the equilibrium is not significantly shifted towards **3a** upon raising the temperature. In contrast to the dihydrogen complex **4**, complexes **5a**, **5b** and **6** do not decompose under 1 atm gas at r.t. both in solution and in the solid state (vide infra) if oxygen is excluded. Since **5a**, **5b** and **6** are labile and readily lose ethylene and acetylene, respectively, NMR spectra had to be recorded under an atmosphere of the respective gas.

Complex **7**, on the other hand, is air stable both in solution and in the solid state even in the absence of CO. The $\nu(\text{CO})$ absorption in Nujol is found at 1961 cm^{-1} . For comparison, in $[\text{RuCp}(\text{PMe}_3)_2(\text{CO})]^+$, $[\text{RuCp}(\text{dippe})(\text{CO})]^+$ (dippe = 1,2-bis(diisopropylphosphino) ethane), $[\text{RuCp}(\text{PPh}_3)_2(\text{CO})]^+$, $[\text{RuCp}(\text{dppm})(\text{CO})]^+$, (dppm = 1,2-bis(diphenylphosphino)methane) the $\nu(\text{CO})$ absorptions (in Nujol) are found at 1961, 1959, 1984, and 1970 cm^{-1} , respectively [14b,16,17].

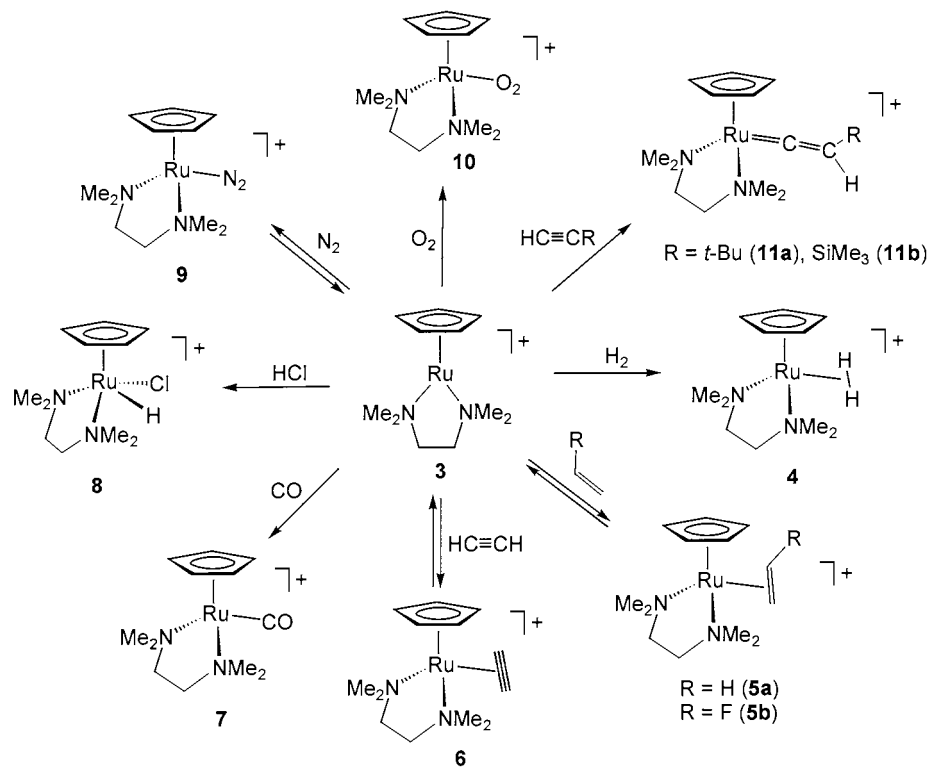
For comparison, the isoelectronic complex $[\text{RuCp}^*(\text{tmeda})]^+$ was reacted with ethylene in CD_2Cl_2 and $^1\text{H-NMR}$ spectra were recorded at various temperatures. While at r.t., no reaction takes place (the solution remains blue); at lower temperatures, the formation of the ethylene complex $[\text{RuCp}^*(\text{tmeda})(\eta^2\text{-CH}_2=\text{CH}_2)]^+$ (**14**) is observed, being in equilibrium with free ethylene. At -60°C , **14** and free ethylene are present in an approximately 5:1 ratio. The color of the solution is still blue. The proton resonances of the ethylene ligand give rise to a multiplet centered at 2.40 ppm indicating that ethylene is not rotating about the metal ligand bond, in contrast to the RuCp analog.

Similar results were obtained for the reaction of $[\text{RuCp}^*(\text{tmeda})]^+$ with acetylene. Addition of acetylene to a CD_2Cl_2 solution of $[\text{RuCp}^*(\text{tmeda})]^+$ at -60°C shows quantitative formation of the η^2 -acetylene adduct $[\text{RuCp}^*(\text{tmeda})(\eta^2\text{-CH}\equiv\text{CH})]^+$ (**15**). In the $^1\text{H-NMR}$ spectrum, singlets at 2.82 and 2.34 ppm for the

tmeda methyl groups point to C_s symmetry suggesting that no ligand exchange between free and coordinated acetylene takes place. Warming the solution above -30°C leads to the disappearance of the signals and formation of a mixture of several products, as judged by the complexity of the $^1\text{H-NMR}$ spectrum.

Cooling a solution of $\text{RuCp}^*(\text{tmeda})^+$ in CD_2Cl_2 and monitoring by $^1\text{H-NMR}$ leads to a broadening of the singlet at 2.88 ppm. Finally, at -90°C , a decoalescence of this signal into two singlets of equal intensity at 3.12 ppm and 2.51 ppm occurs. In order to distinguish whether this signal is assignable to the tmeda methyl groups (12H) or the C_5Me_5 methyl groups (15H), a simple integration was not reliable. A $^1\text{H-}^{13}\text{C}$ COSY spectrum showed a crosspeak for the signals at 48.3 ppm (^{13}C) and 2.88 ppm (^1H) as well as a crosspeak for the signals at 57.1 ppm (^{13}C) and 1.80 ppm (^1H). This clearly shows the ^1H peak at 2.88 ppm should be assigned to the tmeda methyl groups. The C_5Me_5 peaks 1.45 (^1H) and 8.5 (^{13}C) are correlated. No such decoalescence occurs for **3a**, apparently due to less steric repulsion arising from the C_5 ring.

On exposure of **3a** to HCl (one equivalent) in CD_2Cl_2 at -60°C , the color changes immediately from blue to pale yellow due to the formation of a hydride species formulated as $[\text{RuCp}(\text{tmeda})(\text{H})(\text{Cl})]^+$ (**8**). In the $^1\text{H-NMR}$ spectrum the hydride proton is observed as a broad singlet at -4.12 ppm. As in the $^1\text{H-NMR}$ spectrum, four singlets for the tmeda CH_3 groups and



Scheme 2.

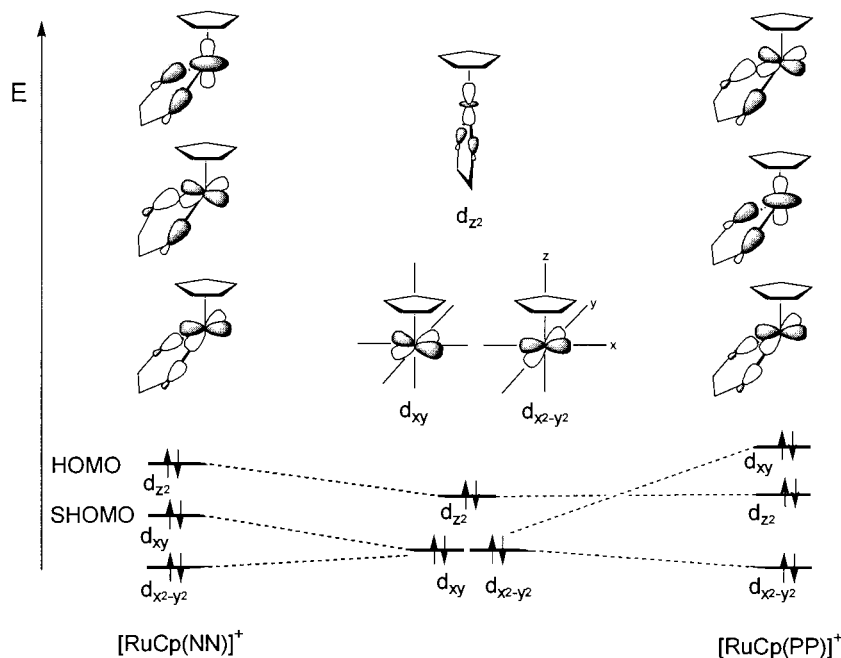


Fig. 2. Qualitative changes in energies for the highest occupied orbitals in $[\text{RuCp}(\text{NN})]^+$ ($\text{NN} = \text{tmeda}$) and $[\text{RuCp}(\text{PP})]^+$ ($\text{PP} = \text{Me}_2\text{PCH}_2\text{CH}_2\text{PMe}_2$) for a planar/pyramidal distortion.

four multiplets for the methylene bridge are observed, it appears that not only a hydride but also a chloride ligand are attached to **3a**, adopting a *cis* arrangement. It has to be mentioned that oxidative addition reactions of CpRu(II) complexes to yield CpRu(IV) complexes have hitherto not been observed in a N-donor environment (in contrast to a P-donor analog). In fact, we have previously shown that the reaction of $[\text{RuCp}^*(\text{tmeda})]^+$ with Br_2 yields the Ru(III) monobromo complex $[\text{RuCp}^*(\text{tmeda})\text{Br}]^+$ rather than the expected Ru(IV) dibromo complex $[\text{RuCp}^*(\text{tmeda})\text{Br}_2]^+$ [6]. Similar results have been obtained by others [18].

In similar fashion, N_2 also reacts with **3a** at -90°C to give quantitatively the dinitrogen complex $[\text{RuCp}(\text{tmeda})(\text{N}_2)]^+$ (**9**). In the course of this reaction, yellow needles are formed. The $^1\text{H-NMR}$ spectrum of the remaining solution shows a shift of all proton resonances relative to **3a** but not the expected change from C_{2v} to C_s symmetry. This clearly indicates that even at -90°C **9** is substitutionally labile with a fast exchange between bound and free N_2 . Interestingly, the formation of **9** is reversible. While at low temperature, the formation of **9** is favored; at ambient temperature, the equilibrium is completely shifted towards **3a** and free N_2 . The instability of **9** at r.t. prevented the recording of an IR spectrum. A similar dinitrogen adduct has been reported for the reaction of the 16 e complexes $[\text{FeCp}(\text{dippe})]^+$, $[\text{RuCp}(\text{dippe})]^+$, and $[\text{RuCp}^*(\text{dippe})]^+$ with N_2 but not with $[\text{FeCp}^*(\text{dippe})]^+$ and $[\text{RuCp}^*(\text{tmeda})]^+$ [1,14].

Finally, on treatment of **3a** with O_2 at -60°C , the color changes to pale yellow due to the formation of $[\text{RuCp}(\text{tmeda})(\text{O}_2)]^+$ (**10**) in essentially quantitative yield. In the $^1\text{H-NMR}$ spectrum, the expected change from C_{2v} to C_s symmetry is observed showing two distinct singlets and multiplets for the tmeda CH_3 and CH_2 protons, respectively. It is not clear at present whether a d^5 Ru(III) superoxo or a d^4 Ru(IV) peroxo complex is dealt with. The diamagnetic behavior of **10** would be consistent with both descriptions since, in the first case, magnetic coupling between the metal ($S = \frac{1}{2}$) and the superoxide ligand ($S = \frac{1}{2}$) may occur resulting in a ground state with $S = 0$. On warming the solution above -30°C , the color changed from yellow to brown and several paramagnetic materials are formed as indicated by NMR spectroscopy.

Independent of what donor molecule is interacting with $[\text{RuCp}(\text{tmeda})]^+$ in the ground state, nucleophilic attack at the metal center is not possible without a prior planar/pyramidal inversion through bending of the Cp and N–Ru–N planes. In the general case of two-legged piano stool metal d^6 complexes CpMLL' in principle each of the orbitals d_{z^2} , $d_{x^2-y^2}$, and d_{xy} can become the HOMO (Fig. 2), depending on the nature of the ligands L and L', with eventually dramatic differences in chemical behavior. Thus, if a d_{z^2} -type orbital remains the HOMO, rather poor π -basicity can be expected. EHMO calculations suggest that this may be the case for $[\text{RuCp}(\text{tmeda})]^+$ explaining, for instance, why this species is not very susceptible to oxidative additions and the Ru(II)/Ru(IV) couple becomes

inaccessible. Accordingly, the $[\text{RuCp}(\text{tmeda})]^+$ fragment favors a dihydrogen structure over a dihydride complex. If, on the other hand, d_{xy} becomes the HOMO, as demonstrated for $L = L' =$ tertiary phosphines, such species will exhibit good π -donor properties.

2.4. Solid–gas reactions [19]

The reactions of **3a** with the gases H_2 , N_2 , O_2 , CO , ethylene, fluoroethylene, and acetylene have also been carried out as solid–gas reactions. In the case of N_2 , no clean reaction took place, as indicated by the lack of color change and elemental analysis. In a typical experiment, an NMR tube was charged with **3a**, evacuated, and then filled with the respective gas (1 atm). In all cases, the reaction resulted in a color change from blue to yellow within 1 min. An exception is fluoroethylene, which required about 2 h for complete conversion. All products have been characterized by elemental analysis (see Section 4). With the exception of the CO adduct, attempts to characterize these materials in solution by NMR and IR spectroscopy failed, since these are unstable in the absence of the respective gases.

In the case of ethylene, the reversibility of this reaction has been investigated. Evacuation of an NMR tube charged with **5a** and heating the solid to 60°C for 1 h leads to release of the olefin to give again **3a**. Interestingly, if the latter solid **3a** is reacted with CO , more than 10 h are required for complete conversion to **7** as compared to 1 min in the original reaction. This may be explained by the loss of the well-ordered crystal lattice during the process of ligand removal.

2.5. Formation of vinylidene complexes

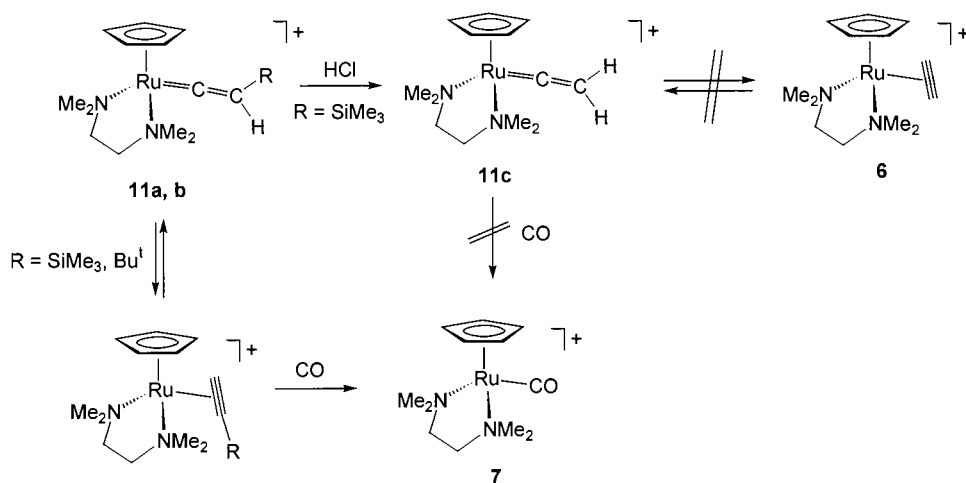
As shown above, the reaction of **3a** with acetylene gives exclusively the η^2 -acetylene complex without any

evidence of rearrangement to a vinylidene complex [20]. On the other hand, both $\text{HC}\equiv\text{CBu}'$ and $\text{HC}\equiv\text{CSiMe}_3$ react within 10 min to yield the respective vinylidene complexes $[\text{RuCp}(\text{tmeda})(=\text{C}=\text{CHBu}')^+]$ (**11a**) and $[\text{RuCp}(\text{tmeda})(=\text{C}=\text{CHSiMe}_3)^+]$ (**11b**) (Scheme 2). Two reasons may account for this R group difference: (i) The vinylidene $\text{Ru}=\text{C}=\text{CH}_2$ is thermodynamically unstable, or (ii) the η^2 acetylene-to-vinylidene rearrangement is kinetically slow. In order to distinguish between these possibilities, the unsubstituted vinylidene complex was synthesized via a different route, viz reaction of **11b** with one equivalent of HCl giving $[\text{RuCp}(\text{tmeda})(=\text{C}=\text{CH}_2)^+]$ (**11c**) and SiClMe_3 (Scheme 3). Since **11c** is stable both in solution and in the solid state (characterized by $^1\text{H-NMR}$ spectroscopy), in the case of **6**, the rearrangement process is apparently kinetically unfavorable.

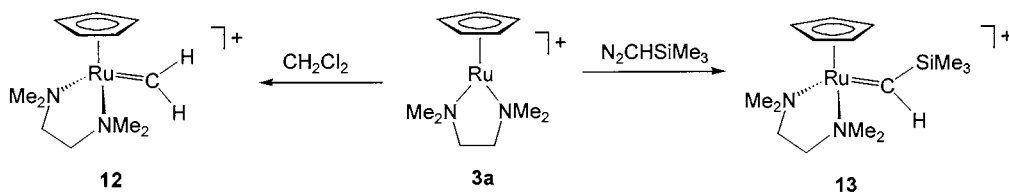
Also, the reverse process, i.e. the rearrangement from vinylidene to the η^2 -alkyne complex, was investigated. Accordingly, the vinylidene complexes **11a** and **11b** were treated with CO at r.t. to afford quantitatively $[\text{RuCp}(\text{tmeda})(\text{CO})]^+$ together with the free alkyne. This reaction goes to completion in less than 48 h. As concerns the reaction mechanism, we propose that CO does not react with the vinylidene complex directly but undergoes substitution with the η^2 -alkyne adduct, which must be in equilibrium with the vinylidene complex as shown in Scheme 3 [20b,21]. The parent vinylidene complex **11c** did not react with CO even after prolonged heating at 40°C . We therefore conclude that the **11c/6** rearrangement process is kinetically unfavorable in both directions.

2.6. Formation of $[\text{RuCp}(\text{tmeda})(=\text{CH}_2)^+]$ by reaction of **3a** with CH_2Cl_2 or CH_2Br_2

Keeping **3a** in a CH_2Cl_2 solution at r.t. for 10 h leads to a color change from blue to brownish yellow due to

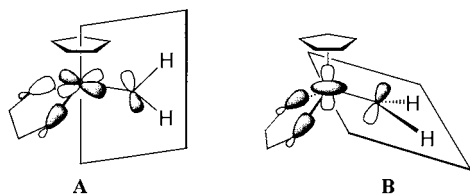


Scheme 3.



Scheme 4.

the formation of the carbene complex $[\text{RuCp}(\text{tmeda})(=\text{CH}_2)]^+$ (**12**) (Scheme 4) [22,23]. The presence of a $=\text{CH}_2$ ligand is clearly indicated by the ^1H - and $^{13}\text{C}\{^1\text{H}\}$ -NMR spectra exhibiting the respective characteristic singlet resonances at 16.89 ppm (2H) and 352.0 ppm. Since we see only one carbene proton signal, even at -90°C in CD_2Cl_2 at 400 MHz, either fast carbene rotation occurs implying a low barrier of rotation or the complex is not dynamic, but with the carbene plane lying perpendicular to the mirror plane of the structure which would leave the two substituent positions equivalent. The first is favored if the HOMO is a d_{xy} orbital (A), while the latter is favored if the HOMO is a d_{z^2} type orbital (B).



With the data at hand, however, we cannot distinguish between these two cases and in any case the rotational barrier may be rather low. Furthermore, the ^1H and $^{13}\text{C}\{^1\text{H}\}$ resonances of the Cp ligand are significantly shifted downfield to 5.43 and 94.1 ppm, respectively, which is indicative of a higher oxidation state of the metal center (cf. 4.10 and 64.9 ppm, respectively, in **3a**). The same product is formed by reaction of **3a** with CH_2Br_2 in *n*-pentane. The fate of the two chlorine, or bromine, atoms, however, remains obscure. Based on ^1H -NMR spectroscopy of the entire reaction solution, **12** and BAR_4^+ are present in a 1:3 ratio. Thus, apparently only 1/3 of **3a** is converted to **12**, whereas the remaining 2/3 are not detected, presumably due to the formation of a paramagnetic Ru(III) species, possibly the cationic Ru(III) complex $[\text{RuCp}(\text{tmeda})\text{Cl}]^+$ (cf. the isoelectronic complex $[\text{RuCp}^*(\text{tmeda})\text{Br}]^+$ has been reported) [6].

Complex **3a** is also able to react directly with a carbene source. Thus, treatment of **3a** with $\text{N}_2\text{CHSiMe}_3$ results in the formation of the cationic carbene complex $[\text{RuCp}(\text{tmeda})(=\text{CHSiMe}_3)]^+$ (**13**) in 79% isolated yield (Scheme 4). The most characteristic feature of the ^1H and $^{13}\text{C}\{^1\text{H}\}$ spectroscopic data are the low-field positions of the carbene hydrogen atom and the carbene

carbon atom, which appear at 20.62 and 352.0 ppm, respectively. We note that structurally related carbene complexes of composition $\text{RuCp}(\text{PPh}_3)(\text{Cl})(=\text{CRR}')$ are known [24].

3. Conclusion

To our knowledge, $[\text{RuCp}(\text{tmeda})]^+$ is the first example of a coordinatively unsaturated RuCp complex. Compared to the corresponding RuCp* analog, $[\text{RuCp}(\text{tmeda})]^+$ is more reactive, yet isolable and hence characterizable despite the absence of bulky and π -donating ligands or any agostic interactions. The increased reactivity the RuCp derivative may be explained in terms of a lowered planar/pyramidal rearrangement barrier as well as a smaller HOMO–LUMO gap. Furthermore, $[\text{RuCp}(\text{NN})]^+$ complexes in contrast to analogous $[\text{RuCp}(\text{PP})]^+$ complexes appear to be poor π -bases making them reluctant to undergo 2 e oxidative additions. Accordingly, the $[\text{RuCp}(\text{tmeda})]^+$ fragment favors a dihydrogen structure over a dihydride complex. In contrast, $[\text{RuCp}^*(\text{tmeda})]^+$ does not even react with H_2 .

4. Experimental

4.1. General

All manipulations were carried out with standard Schlenk and glovebox techniques under purified argon. Benzene, toluene, Et_2O , CH_2Cl_2 , and pentane were dried using appropriate agents, distilled, and stored in gas-tight solvent bulbs. Benzene- d_6 , CD_2Cl_2 , and toluene- d_8 were dried by appropriate methods and vacuum-distilled prior to use. All chemicals were standard reagent grade and used without further purification. Gaseous reagents were purchased from Air Products and used as received. $[\text{RuCp}(\text{CH}_3\text{CN})_3]\text{PF}_6$ and $[\text{RuCp}^*(\text{tmeda})]\text{BAR}_4^+$ were synthesized according to the literature [6a,25]. For the latter, ^1H -NMR (CD_2Cl_2 , -40°C): 7.76 (m, 8H), 7.61 (s, 4H), 2.88 (s, 12H, NMe_2), 1.80 (s, 4H, $\text{NCH}_2\text{CH}_2\text{N}$), 1.45 (s, 15H, C_5Me_5). $^{13}\text{C}\{^1\text{H}\}$ -NMR (CD_2Cl_2 , -40°C): 160.3 (q,

$J_{BC} = 49.6$ Hz), 133.3, 127.4 (q, $J_{CF} = 31.5$ Hz), 123.1 (q, $J_{CF} = 272.3$ Hz), 115.9, 69.3 (C_5Me_5), 57.1, 48.3, 8.5 (C_5Me_5). 1H -, $^{13}C\{^1H\}$ -, $^{31}P\{^1H\}$ -, and $^{19}F\{^1H\}$ -NMR spectra were recorded on either Bruker 250AC, Varian Gemini 300 or Varian INOVA 400 spectrometers and were referenced to $SiMe_4$ and H_3PO_4 (85%). $^{19}F\{^1H\}$ -NMR chemical shifts were externally referenced to CF_3COOH in benzene. Infrared spectra were recorded on a Nicolet 510P FTIR spectrometer. Elemental analyses were performed by Microanalytical Laboratories, University of Vienna.

4.2. Synthesis

4.2.1. $[RuCp(tmeda)(CH_3CN)]PF_6$ (**1**)

$[RuCp(CH_3CN)_3]PF_6$ (349 mg, 0.803 mmol) and *tmeda* (112.1 mg, 0.964 mmol) in Et_2O (15 ml) were stirred at r.t. for 15 h. After evaporation of the solvent, the pale yellow solid was dried under vacuum. Yield:

Table 1
Crystallographic data for $[(C_5H_5)Ru(tmeda)][B(C_6H_3(CF_3)_2)_4]$

Formula	$C_{43}H_{33}BF_{24}N_2Ru$
<i>a</i> (Å)	17.405(1)
<i>b</i> (Å)	19.453(2)
<i>c</i> (Å)	26.918(2)
<i>V</i> (Å ³)	9113.78
<i>Z</i>	8
Formula weight	1145.59
Space group	<i>Pbca</i>
<i>T</i> (°C)	−170
λ (Å)	0.71069
D_{calc} (g cm ^{−3})	1.670
μ (Mo–K α) (cm ^{−1})	4.8
<i>R</i> ^a	0.0564
<i>R</i> _w ^b	0.0471

$$^a R = \frac{\sum |F_o| - |F_c|}{\sum |F_o|}$$

$$^b R_w = \frac{\sum w(|F_o| - |F_c|)^2}{\sum w|F_o|^2} \text{ where } w = 1/\sigma^2(|F_o|).$$

Table 2
Selected bond distances (Å) and angles (°) for $[(C_5H_5)Ru(tmeda)][B(C_6H_3(CF_3)_2)_4]$

Ru(1)–N(2)	2.142(6)	N(2)–C(3)	1.496(11)
Ru(1)–N(5)	2.163(8)	N(2)–C(6)	1.497(10)
Ru(1)–C(10)	2.109(15)	N(2)–C(7)	1.472(9)
Ru(1)–C(11)	2.052(12)	N(5)–C(4)	1.503(13)
Ru(1)–C(12)	2.106(12)	N(5)–C(8)	1.459(12)
Ru(1)–C(13)	2.118(13)	N(5)–C(9)	1.460(12)
Ru(1)–C(14)	2.059(12)	C(3)–C(4)	1.473(13)
N(2)–Ru(1)–N(5)	80.85(27)	Ru(1)–N(5)–C(8)	115.7(7)
Ru(1)–N(2)–C(3)	108.6(5)	Ru(1)–N(5)–C(9)	109.5(7)
Ru(1)–N(2)–C(6)	103.7(5)	C(4)–N(5)–C(8)	105.9(8)
Ru(1)–N(2)–C(7)	116.9(5)	C(4)–N(5)–C(9)	109.7(9)
C(3)–N(2)–C(6)	110.2(7)	C(8)–N(5)–C(9)	107.4(8)
C(3)–N(2)–C(7)	109.4(7)	N(2)–C(3)–C(4)	110.5(8)
C(6)–N(2)–C(7)	107.9(6)	N(5)–C(4)–C(3)	108.7(9)
Ru(1)–N(5)–C(4)	108.5(6)		

350 mg (93%). Anal. Calc. for $C_{13}H_{24}F_6N_3PRu$: C, 33.34; H, 5.16; N, 8.97. Found: C, 33.44; H, 5.27; N, 9.09%. 1H -NMR (−30°C, acetone-*d*₆): 4.10 (s, 5H), 3.29 (s, 6H), 2.75 (s, 6H), 2.69 (m, 2H), 2.63 (s, 3H), 2.42 (m, 2H). $^{13}C\{^1H\}$ -NMR (δ , acetone-*d*₆, −30°C): CN not observed, 68.5 (s, 5C, Cp), 62.6 (s, 2C, NCH₃), 59.0 (s, 2C, CH₂), 54.7 (s, 2C, NCH₃), 4.6 (CH₃). IR (KBr, cm^{−1}): 2254 (s, ν_{CN}).

4.2.2. $RuCp(tmeda)Cl$ (**2**)

To a solution of **1** (350 mg, 0.747 mmol) in CH_2Cl_2 (15 ml) NEt_4Cl (300 mg, 1.810 mmol) was added. After stirring of the orange solution for 15 min at r.t., the solvent was removed and the residue was redissolved in CH_2Cl_2 (5 ml). On addition of Et_2O (20 ml) a white precipitate of NEt_4PF_6 was formed and removed by filtration. The solvent was then removed and the analytically pure product dried in vacuo. Yield: 195 mg (82%). Anal. Calc. for $C_{11}H_{21}ClN_2Ru$: C, 41.57; H, 6.66; N, 8.81. Found: C, 41.68; H, 6.52; N, 8.97%. 1H -NMR (25°C, CD_2Cl_2): 3.65 (s, 5H), 3.23 (s, 6H), 2.78 (s, 6H), 2.30 (s, 4H).

4.2.3. $[RuCp(tmeda)]BAR'_4$ (**3a**)

Compound **2** (74 mg, 0.233 mmol) and $NaBAR'_4$ (206 mg, 0.233 mmol) in fluorobenzene (3 ml) were stirred at r.t. for 15 h. After removal of $NaCl$, the blue product was precipitated by addition of *n*-pentane. The product was collected on a glass frit and dried under vacuum. Yield: 230 mg (86%). Anal. Calc. for $C_{43}H_{33}BF_{24}N_2Ru$: C, 45.08; H, 2.90; N, 2.45. Found: C, 45.23; H, 2.92; N, 2.70%. 1H -NMR (25°C, CD_2Cl_2): 7.74 (m, 8H), 7.59 (m, 4H), 4.02 (s, 5H), 3.45 (bs, 12H), 2.49 (bs, 4H). $^{13}C\{^1H\}$ -NMR (CD_3NO_2 , −30°C): 162.4 (q, BAR'_4 , $J_{CB} = 51.1$ Hz), 134.9 (s, BAR'_4), 129.8 (q, BAR'_4 , $J_{FC} = 29.8$ Hz), 126.1 (q, BAR'_4 , $J_{FC} = 144.2$ Hz), 117.9 (s, BAR'_4), 65.9 (s, 5C, Cp), 62.4 (s, 4C, NCH₃), 62.1 (s, 2C, CH₂).

4.2.4. Structure determination of $[(C_5H_5)Ru(tmeda)][B(C_6H_3(CF_3)_2)_4]$

A fragment of a crystal was transferred to the goniostat and cooled to −173°C. The sample was handled under argon during all phases until transfer to the goniostat. A systematic search of a limited hemisphere of reciprocal space was used to determine that the crystal possessed orthorhombic symmetry with systematic absences corresponding to the unique space group *Pbca* (Tables 1 and 2). Subsequent solution and refinement confirmed this choice. The data were collected ($6^\circ < 2\theta < 50^\circ$) using a standard moving crystal-moving detector technique with fixed backgrounds at each extreme of the scan. Data were corrected for absorption, Lorentz and polarization effects and equivalent reflections averaged. The structure was readily solved using direct methods (MULTAN-78) and Fourier techniques.

In spite of an absorption correction, several of the carbon atoms in the anion refined to non-positive definite thermal parameters, as did one of the carbon atoms in the Cp ring. For this reason, all carbon atoms in the anion, and C(10) were assigned isotropic thermal parameters for the refinement. Hydrogen atoms were placed in fixed, idealized positions for the final cycles of refinement. A second crystal was also examined to try to improve the quality of the data. In spite of being a better crystal, the refinement of these data was inferior to the data reported herein. A final difference Fourier map was featureless, the largest peak of intensity $0.88 \text{ e } \text{Å}^{-3}$.

4.2.5. [RuCp(tmeda)]PF₆ (**3b**)

4.2.5.1. Method a. Compound **2** (46.7 mg, 0.147 mmol) and TlPF₆ (52 mg, 0.147 mmol) were dissolved in tetrahydrofuran (10 ml) and stirred for 30 min at r.t., wherein the color of the solution turned bright orange and a white precipitate formed. After filtration through Celite, the solvent was removed in vacuo and the color of the solid turned blue. Yield: 51.5 mg (82%).

4.2.5.2. Method b. Compound **1** (50 mg, 0.107 mmol) was heated at 150°C under reduced pressure (ca 10^{-2} atm) for 1 h, whereupon the color changed from yellow to deep blue. The solubility of **3b** is extremely poor in CD₂Cl₂ but good in CD₃NO₂. ¹H- and ¹³C{¹H}-NMR spectra are virtually identical to those of **3a**.

4.2.6. [RuCp(tmeda)(η²-H₂)]BAR'₄ (**4**)

An NMR tube was charged with **3a** (15.4 mg, 0.0134 mmol) and CD₂Cl₂ (0.5 ml). On a gas line, H₂ (0.054 mmol) was added at -200°C. After warming up the solution to -90°C, the color changed to greenish blue and a ¹H-NMR spectrum was recorded. ¹H-NMR (-90°C, CD₂Cl₂): 7.74 (m, 8H), 7.55 (m, 4H), 5.33 (s, 5H), 3.03 (s, 6H), 2.83 (s, 6H), 2.71 (m, 2H), 2.36 (m, 2H), -3.6 (s, 2H). T_1 (-90°C, CD₂Cl₂) = 10.2 ± 0.4 ms.

4.2.7. [RuCp(tmeda)(η²-CH₂=CH₂)]BAR'₄ (**5a**)

An NMR tube was charged with **3a** (18.6 mg, 0.0162 mmol) and CD₂Cl₂ (0.5 ml). On a gas line, ethylene (0.054 mmol) was added at -200°C. After warming up the solution to -60°C, the color changed to pale yellow and a ¹H-NMR spectrum was recorded. ¹H-NMR (-60°C, CD₂Cl₂): 7.76 (m, 8H), 7.56 (m, 4H), 4.49 (s, 5H), 4.01 (bs, 4H), 3.00 (s, 6H), 2.91 (m, 2H), 2.32 (s, 6H), 2.24 (m, 2H). ¹H-NMR (25°C, CD₂Cl₂): 7.74 (m, 8H), 7.58 (m, 4H), 5.35 (bs, 4H, free and bound ethylene), 4.53 (s, 5H), 2.71 (bs, 12H), 2.46 (bs, 4H).

4.2.8. [RuCp(tmeda)(η²-CHF=CH₂)]BAR'₄ (**5b**)

An NMR tube was charged with **3a** (18.6 mg, 0.0162 mmol) and CD₂Cl₂ (0.5 ml). On a gas line fluoroethylene (0.054 mmol) was added at -200°C. After warming up the solution to -60°C, the color changed to pale yellow and a ¹H-NMR spectrum was recorded. ¹H-NMR (-60°C, CD₂Cl₂): 7.73 (m, 8H), 7.56 (m, 4H), 6.63 (m, 1H), 4.83 (m, 1H), 4.70 (s, 5H), 4.52 (d, 1H), 3.05 (s, 3H), 2.93 (s, 3H), 2.60 (m, 2H), 2.44 (s, 3H), 2.25 (m, 2H), 2.21 (s, 3H). ¹⁹F{¹H}-NMR (-60°C, CD₂Cl₂): -51.3 (s, BAR'₄), -105.28 (m, C₂H₃F).

4.2.9. [RuCp(tmeda)(η²-CH≡CH)]BAR'₄ (**6**)

An NMR tube was charged with **3a** (14.8 mg, 0.0129 mmol) and CD₂Cl₂ (0.5 ml). On a gas line, acetylene (0.054 mmol) was added at -200°C. After warming up the solution to -60°C, the color changed to pale yellow and a ¹H-NMR spectrum was recorded. ¹H-NMR (-60°C, CD₂Cl₂): 7.73 (m, 8H), 7.55 (m, 4H), 5.23 (s, 2H), 4.55 (s, 5H), 3.00 (s, 6H), 2.48 (m, 2H), 2.34 (s, 6H), 2.08 (m, 2H). ¹H-NMR (25°C, CD₂Cl₂): 7.73 (m, 8H), 7.55 (m, 4H), 4.55 (s, 5H), 2.74 (bs, 12H), 2.32 (bs, 4H), 3.10–1.90 (bs, 2H, free and bound acetylene).

4.2.10. [RuCp(tmeda)(CO)]BAR'₄ (**7**)

An NMR tube was charged with **3a** (15.4 mg, 0.0134 mmol) in CD₂Cl₂ (0.5 ml). On a gas line, CO (1 atm) was added and the reaction was allowed to proceed at r.t. for 1 min, whereupon the blue solid turned yellow. Then the tube was evacuated again and the product dissolved in CD₂Cl₂. ¹H-NMR (25°C, CD₂Cl₂): 7.74 (m, 8H), 7.58 (m, 4H), 4.93 (s, 5H), 3.00 (s, 6H), 2.99 (s, 6H), 2.79 (m, 4H). ¹³C{¹H}-NMR (25°C, CD₃NO₂): 203.8.6 (CO), 160.0 (q, BAR'₄, $J_{CB} = 50.0$ Hz), 134.0 (s, BAR'₄), 128.0 (q, BAR'₄, $J_{FC} = 29.8$ Hz), 124.3 (s, C_z), 124.1 (q, BAR'₄, $J_{FC} = 143.1$ Hz), 116.8 (s, BAR'₄), 84.0 (Cp), 64.4 (CH₂), 61.9 (CH₃), 60.3 (CH₃). IR (CH₂Cl₂, 25°C): 1968 cm⁻¹ (ν_{CO}). IR (Nujol, 25°C): 1961 cm⁻¹.

4.2.11. [RuCp(tmeda)(H)(Cl)]BAR'₄ (**8**)

An NMR tube was charged with **3a** (14.8 mg, 0.0129 mmol) and CD₂Cl₂ (0.5 ml). On a gas line, HCl (0.054 mmol) was added at -200°C. After warming up the solution to -60°C, the color changed to pale yellow and a ¹H-NMR spectrum was recorded. ¹H-NMR (-60°C, CD₂Cl₂): 7.73 (m, 8H), 7.56 (m, 4H), 5.11 (s, 5H), 3.15 (s, 3H), 3.07 (s, 6H), 2.90–2.70 (m, 4H), 2.71 (s, 3H), -4.12 (s, 1H).

4.2.12. [RuCp(tmeda)(N₂)]BAR'₄ (**9**)

An NMR tube was charged with **3a** (14.8 mg, 0.0129 mmol) and CD₂Cl₂ (0.5 ml). On a gas line, N₂ (0.054 mmol) was added at -200°C. After warming up the solution to -60°C, the color changed to pale yellow

Table 3
Solid–gas reactions of $[\text{RuCp}(\text{tmeda})(\text{O}_2)]\text{BAr}'_4$

Compound	Time	Color	Molecular formula	Calc.			Found		
				C	H	N	C	H	N
4	<1 min	Green	$\text{C}_{43}\text{H}_{35}\text{BF}_{24}\text{N}_2\text{Ru}$	45.00	3.07	2.44	44.83	3.15	2.32
5a	<1 min	Yellow	$\text{C}_{45}\text{H}_{37}\text{BF}_{24}\text{N}_2\text{Ru}$	46.05	3.18	2.39	46.17	3.14	2.47
5b	2 h	Yellow	$\text{C}_{45}\text{H}_{36}\text{BF}_{25}\text{N}_2\text{Ru}$	45.36	3.05	2.35	45.10	3.12	2.52
6	<1 min	Yellow	$\text{C}_{45}\text{H}_{35}\text{BF}_{24}\text{N}_2\text{Ru}$	46.13	3.01	2.39	46.02	3.08	2.49
7	<1 min	Yellow	$\text{C}_{44}\text{H}_{33}\text{BF}_{24}\text{N}_2\text{ORu}$	45.03	2.83	2.39	44.95	2.89	2.62
10	<1 min	Orange	$\text{C}_{43}\text{H}_{33}\text{BF}_{24}\text{N}_2\text{O}_2\text{Ru}$	43.86	2.82	2.38	43.69	2.79	2.44

and yellow needles formed. A $^1\text{H-NMR}$ spectrum was recorded at this temperature. $^1\text{H-NMR}$ (-60°C , CD_2Cl_2): 7.68 (m, 8H), 7.52 (m, 4H), 4.39 (s, 5H, Cp), 2.85 (bs, 12H, NMe_2), 2.56 (bs, 4H, NCH_2).

4.2.13. $[\text{RuCp}(\text{tmeda})(\text{O}_2)]\text{BAr}'_4$ (**10**)

An NMR tube was charged with **3a** (14.8 mg, 0.0129 mmol) and CD_2Cl_2 (0.5 ml). On a gas line, O_2 (0.054 mmol) was added at -200°C . After warming up the solution to -60°C , the color changed to pale yellow. A $^1\text{H-NMR}$ spectrum was recorded at this temperature. $^1\text{H-NMR}$ (-60°C , CD_2Cl_2): 7.74 (s, 8H), 7.57 (s, 4H), 5.56 (s, 5H), 2.76 (s, 6H), 2.73 (s, 6H), 2.64–2.57 (m, 4H).

4.2.14. Solid–gas reactions

In a typical experiment, an NMR tube charged with 15 mg of **3a**, was evacuated and filled with reactant (1 atm). A color change from blue to orange–yellow indicated the completion of the reaction (see Table 3).

4.2.15. $[\text{RuCp}(\text{tmeda})(=\text{C}=\text{CHBu}')] \text{BAr}'_4$ (**11a**)

Compound **3a** (15.8 mg, 0.0138 mmol) and $\text{HC}\equiv\text{CBu}'$ (1.13 mg, 0.0138 mmol) were dissolved in fluorobenzene (0.5 ml) and stirred at r.t. for 10 min. The orange solution was evaporated to dryness and the precipitate washed with pentane. Anal. Calc. for $\text{C}_{49}\text{H}_{43}\text{BF}_{24}\text{N}_2\text{Ru}$: C, 47.94; H, 3.53; N, 2.28. Found: C, 47.74; H, 3.46; N, 2.48%. $^1\text{H-NMR}$ (25°C , CD_2Cl_2): 7.72 (s, 8H), 7.56 (s, 4H), 5.14 (s, 5H), 3.80 (s, 1H), 2.95 (m, 2H), 2.91 (s, 6H), 2.74 (m, 2H), 2.76 (s, 6H), 1.16 (s, 9H). $^{13}\text{C}\{^1\text{H}\}$ -NMR (25°C , CD_2Cl_2): 333.6 (C_α), 160.0 (q, BAr'_4 , $J_{\text{CB}} = 50.0$ Hz), 134.0 (s, BAr'_4), 128.0 (q, BAr'_4 , $J_{\text{FC}} = 29.8$ Hz), 124.3 (s, C_β), 124.1 (q, BAr'_4 , $J_{\text{FC}} = 143.1$ Hz), 116.8 (s, BAr'_4), 88.0 (Cp), 63.4 (tmeda, CH_2), 59.9 (tmeda, CH_3), 59.8 (tmeda, CH_3), 43.8 (^iBu , C), 31.3 (^iBu , CH_3).

4.2.16. $[\text{RuCp}(\text{tmeda})(=\text{C}=\text{CHSiMe}_3)] \text{BAr}'_4$ (**11b**)

This complex was prepared analogously to **11a** using $\text{HC}\equiv\text{CSiMe}_3$ as the terminal acetylene. Anal. Calc. for $\text{C}_{48}\text{H}_{43}\text{BF}_{24}\text{N}_2\text{RuSi}$: C, 46.35; H, 3.48; N, 2.25. Found: C, 46.29; H, 3.39; N, 2.43%. $^1\text{H-NMR}$ (25°C , CD_2Cl_2): 7.72 (s, 8H), 7.56 (s, 4H), 5.06 (s, 5H), 3.41 (s, 1H), 2.95

(s, 6H), 2.91 (m, 2H), 2.80 (s, 6H), 2.72 (m, 2H), 0.18 (s, 9H).

4.2.17. $[\text{RuCp}(\text{tmeda})(=\text{C}=\text{CH}_2)] \text{BAr}'_4$ (**11c**)

To a solution of **11b** (13.4 mg, 0.0108 mmol) in fluorobenzene gaseous HCl (0.0108 mmol) was added at -100°C . The solution was allowed to warm slowly and stirred for 10 min at r.t. After removal of the solvent in vacuo, the residue was washed twice with *n*-pentane and dried in vacuo. Anal. Calc. for $\text{C}_{45}\text{H}_{35}\text{BF}_{24}\text{N}_2\text{Ru}$: C, 46.13; H, 3.01; N, 2.39. Found: C, 46.18; H, 3.04; N, 2.51%. $^1\text{H-NMR}$ (25°C , CD_2Cl_2): 7.72 (s, 8H), 7.56 (s, 4H), 5.22 (s, 5H), 3.31 (s, 2H), 3.10 (m, 2H), 2.94 (s, 6H), 2.78 (m, 2H), 2.76 (s, 6H).

4.2.18. $[\text{RuCp}(\text{tmeda})(=\text{CH}_2)] \text{BAr}'_4$ (**12**)

Compound **3a** (18.9 mg, 0.0165 mmol) was stirred in CH_2Cl_2 solution for 10 h at r.t., wherein the color changed from blue to brownish yellow. The solvent was evaporated and the residue dried in vacuo. $^1\text{H-NMR}$ (-20°C , CD_2Cl_2): 16.89 (s, 2H), 7.77 (s, 8H), 7.61 (s, 4H), 5.43 (s, 5H), 3.45 (m, 2H), 2.95 (m, 2H), 2.68 (s, 6H), 2.52 (s, 6H). $^{13}\text{C}\{^1\text{H}\}$ -NMR (-20°C , CD_2Cl_2): 352.0 (C_α), 161.6 (q, BAr'_4 , $J_{\text{CB}} = 50.0$ Hz), 134.9 (s, BAr'_4), 129.0 (q, BAr'_4 , $J_{\text{FC}} = 29.8$ Hz), 124.8 (q, BAr'_4 , $J_{\text{FC}} = 143.1$ Hz), 116.8 (s, BAr'_4), 94.1 (Cp), 64.8 (tmeda, CH_2), 61.4 (tmeda, CH_3), 61.1 (tmeda, CH_3).

Complex **12** is also accessible by treatment of **3a** with CH_2Br_2 (two equivalents) in pentane for 2 h at r.t.

4.2.19. $[\text{RuCp}(\text{tmeda})(=\text{CHSiMe}_3)] \text{BAr}'_4$ (**13**)

Compound **3a** (45.5 mg, 0.0397 mmol) was dissolved in CH_2Cl_2 and $\text{N}_2\text{CHSiMe}_3$ (1 M in hexane, 0.0397 mmol) was added. The solution turned light green immediately. After evaporation of the solvent, the residue was redissolved in CH_2Cl_2 (1 ml) and the product precipitated by addition of pentane. Yield: 38.6 mg (79%). Anal. Calc. for $\text{C}_{47}\text{H}_{43}\text{BF}_{24}\text{N}_2\text{RuSi}$: C, 45.83; H, 3.52; N, 2.27. Found: C, 45.67; H, 3.67; N, 2.44%. $^1\text{H-NMR}$ (25°C , CD_2Cl_2): 20.62 (s, 1H), 7.72 (s, 8H), 7.56 (s, 4H), 5.49 (s, 5H), 3.38 (m, 2H), 2.81 (m, 2H), 2.56 (s, 6H), 2.48 (s, 6H). $^{13}\text{C}\{^1\text{H}\}$ -NMR (25°C , CD_2Cl_2): 352.0 (C_α), 162.1 (q, BAr'_4 , $J_{\text{CB}} = 50.0$ Hz), 135.2 (s, BAr'_4), 129.4 (q, BAr'_4 , $J_{\text{FC}} = 29.8$ Hz), 125.2

(q, BAR'_4 , $J_{\text{FC}} = 143.1$ Hz), 117.9 (s, BAR'_4), 93.0 (Cp), 64.7 (tmeda, CH_2), 61.9 (tmeda, CH_3), 60.6 (tmeda, CH_3), -1.3 (SiMe_3).

4.2.20. $[\text{RuCp}^*(\text{tmeda})(\eta^2\text{-CH}_2=\text{CH}_2)]\text{BAR}'_4$ (**14**)

An NMR tube was charged with $[\text{RuCp}^*(\text{tmeda})]\text{BAR}'_4$ (14.8 mg, 0.0129 mmol) and CD_2Cl_2 (0.5 ml). On a gas line, ethylene (0.054 mmol) was added at -200°C . After warming up the solution to -60°C , the color changed to pale yellow and a $^1\text{H-NMR}$ spectrum was recorded. $^1\text{H-NMR}$ (-60°C , CD_2Cl_2): 7.72 (m, 8H), 7.55 (m, 4H), 3.15 (m, 2H), 2.77 (s, 6H), 2.70 (m, 2H), 2.40 (m, 4H), 2.18 (s, 6H), 1.32 (s, 15H).

4.2.21. $[\text{RuCp}^*(\text{tmeda})(\eta^2\text{-CH}\equiv\text{CH})]\text{BAR}'_4$ (**15**)

An NMR tube was charged with $[\text{RuCp}^*(\text{tmeda})]\text{BAR}'_4$ (14.8 mg, 0.0129 mmol) and CD_2Cl_2 (0.5 ml). On a gas line, acetylene (0.054 mmol) was added at -200°C . After warming up the solution to -60°C , the color changed to pale yellow and a $^1\text{H-NMR}$ spectrum was recorded. $^1\text{H-NMR}$ (-60°C , CD_2Cl_2): 7.73 (m, 8H), 7.56 (m, 4H), 2.82 (s, 6H), 2.34 (s, 6H), 3.2–2.0 (m, 4H), 2.03 (2H, free and bound acetylene), 1.36 (s, 15H).

5. Supplementary material

Listings of atomic coordinates, anisotropic temperature factors, bond lengths and angles for **3a** are available from the authors upon request.

Acknowledgements

Financial support by the US National Science Foundation and by the 'Fonds zur Förderung der wissenschaftlichen Forschung' (project no. J1535-CHE).

References

- [1] A. de la Jara Leal, M. Jimenez-Tenorio, M.C. Puerta, P. Valerga, *Organometallics* 14 (1995) 3839.
- [2] P. Hamon, L. Toupet, J.R. Hamon, C. Lapinte, *Organometallics* 15 (1996) 10.
- [3] U. Koelle, J. Kossakowski, *Angew. Chem. Int. Ed. Engl.* 29 (1990) 773; M.E. Smith, F.J. Hollander, R.A. Anderson, *Angew. Chem.* 32 (1993) 1294.
- [4] K. Mauthner, C. Slugovc, K. Mereiter, R. Schmid, K. Kirchner, *Organometallics* 16 (1997) 1956.
- [5] C.L. Gross, G.S. Girolami, *J. Am. Chem. Soc.* 120 (1998) 6605.
- [6] (a) C. Gemel, K. Mereiter, R. Schmid, K. Kirchner, *Organometallics* 16 (1997) 5601. (b) C. Gemel, V.N. Sapunov, K. Mereiter, M. Ferencic, R. Schmid, K. Kirchner, *Inorg. Chim. Acta* 286 (1999) 114.
- [7] W. Luginbühl, P. Zbinden, P.A. Pittet, T. Armbruster, H.-B. Bürgi, A.E. Merbach, A. Ludi, *Inorg. Chem.* 30 (1991) 2350.
- [8] M.H. Wang, U. Englert, U. Kölle, *J. Organomet. Chem.* 453 (1993) 127.
- [9] For Ru 16-electron complexes see: (a) B.K. Campion, R.H. Heyn, D.D. Tilley, *J. Chem. Soc. Chem. Commun.* (1988) 278. (b) T.J. Johnson, K. Foltz, W.E. Streib, J.D. Martin, J.C. Huffman, S.A. Jackson, O. Eisenstein, K.G. Caulton, *Inorg. Chem.* 34 (1995) 488. (c) E. Lindner, M. Haustein, H.A. Mayer, K. Gierling, R. Fawzi, M. Steinmann, *Organometallics* 14 (1995) 2246. (d) J.-P. Sutter, S.L. James, P. Steenwinkel, T. Karlen, D.M. Grove, N. Veldman, W.J.J. Smeets, A.L. Spek, G. van Koten, *Organometallics* 15 (1996) 941. (e) K. Mashima, H. Kaneyoshi, S. Kaneko, A. Mikami, K. Tani, A. Nakamura, *Organometallics* 16 (1997) 1016. (f) T. Braun, M. Laubender, O. Gevert, H. Werner, *Chem. Ber.* 130 (1997) 559. (g) G. Jia, H.M. Lee, H.P. Xia, I.D. Williams, *Organometallics* 15 (1996) 5453. (h) T. Karlen, P. Dani, D.M. Grove, P. Steenwinkel, G. van Koten, *Organometallics* 15 (1996) 5687. (i) J. Huang, E.D. Stevens, S.P. Nolan, J.L. Peterson, *J. Am. Chem. Soc.* 121 (1999) 2674.
- [10] F.L. Joslin, M.P. Johnson, J.T. Mague, D.M. Roundhill, *Organometallics* 10 (1991) 2781.
- [11] For Ru- $\eta^1(\text{O})\text{-CF}_3\text{SO}_3$ complexes see: (a) A.C. Ontko, J.F. Houllis, R.C. Schnabel, D.M. Roddick, T.P. Fong, A.J. Lough, R.H. Morris, *Organometallics* 17 (1999) 5467. (b) K. Mauthner, C. Slugovc, K. Mereiter, R. Schmid, K. Kirchner, *Organometallics* 16 (1997) 1956. (c) C. Gemel, D. Kalt, K. Mereiter, V.N. Sapunov, R. Schmid, K. Kirchner, *Organometallics* 16 (1997) 427. (d) M.J.A. Kraakman, B. de Klerk-Engels, P.P.M. de Lange, K. Vrieze, W.J.J. Smeets, A.L. Spek, *Organometallics* 11 (1992) 3774. (e) P.W. Plosser, J.C. Gallucci, A. Wojcicki, *Inorg. Chem.* 31 (1992) 2376. (f) I. del Rio, R.A. Gossage, M.S. Hannu, M. Lutz, A.L. Spek, G. van Koten, *Organometallics* 18 (1999) 1097.
- [12] (a) D. Huang, J.C. Huffman, J.C. Bollinger, O. Eisenstein, K.G. Caulton, *J. Am. Chem. Soc.* 119 (1997) 7398. (b) B.A. Arndtsen, R.G. Bergman, *Science* 270 (1995) 1970.
- [13] (a) P.G. Jessop, R.H. Morris, *Coord. Chem. Rev.* 121 (1992) 155. (b) D.M. Heinekey, W.J. Oldham, *J. Chem. Rev.* 93 (1993) 913. (c) R.H. Crabtree, *Angew. Chem. Int. Ed. Engl.* 32 (1993) 789.
- [14] (a) G. Jia, C.P. Lau, *J. Organomet. Chem.* 565 (1998) 37. (b) I. de los Rios, M.J. Tenorio, J. Padilla, M.C. Puerta, P. Valerga, *Organometallics* 15 (1996) 4565. (c) G. Jia, R.H. Morris, *J. Am. Chem. Soc.* 113 (1991) 875. (d) F.M. Conroy-Lewis, S.J. Simpson, *J. Organomet. Chem.* (1987) 1675.
- [15] B. de Klerk-Engels, J.G.P. Delis, J.M. Ernsting, C.J. Elsevier, H.W. Frühauf, D.J. Stufkens, K. Vrieze, K. Goubitz, J. Fraanje, *Inorg. Chim. Acta* 240 (1995) 273.
- [16] M.I. Bruce, F.S. Wong, B.W. Skelton, A.H. White, *J. Chem. Soc. Dalton Trans.* (1981) 1398.
- [17] G.S. Ashby, M.I. Bruce, I.B. Tomkins, R.C. Wallis, *Aust. J. Chem.* 32 (1979) 1003.
- [18] B.R. Manzano, F.A. Jalon, F.J. Lahoz, B. Chaudret, D.d. Montauzon, *J. Chem. Soc. Dalton Trans.* (1992) 977.
- [19] M. Oliván, A.V. Marchenko, J.N. Coalter, K.G. Caulton, *J. Am. Chem. Soc.* 119 (1997) 8389.
- [20] (a) M.I. Bruce, *Chem. Rev.* 91 (1991) 197. (b) C. Slugovc, V.N. Sapunov, P. Wiede, K. Mereiter, R. Schmid, K. Kirchner, *J. Chem. Soc. Dalton Trans.* (1997) 4209. (c) I. de los Rios, M.J. Tenorio, M.C. Puerta, P. Valerga, *J. Am. Chem. Soc.* 119 (1997) 6529. (d) J.R. Lompfrey, J.R. Selegue, *J. Am. Chem. Soc.* 114 (1992) 5518. (e) Y. Wakatsuki, N. Koga, H. Werner, K. Morokuma, *J. Am. Chem. Soc.* 119 (1997) 360.

- [21] (a) M. Martin, O. Gevert, H. Werner, J. Chem. Soc. Dalton Trans. (1996) 2275. (b) C. Bianchini, G. Purches, F. Zanobini, M. Peruzzini, Inorg. Chim. Acta 272 (1998) 1.
- [22] K.J. Bradd, B.T. Heaton, C. Jacob, J.T. Sampanthar, A. Steiner, J. Chem. Soc. Dalton Trans. (1999) 1109.
- [23] M. Oliván, K.G. Caulton, Inorg. Chem. 38 (1999) 566.
- [24] T. Braun, O. Gevert, H. Werner, J. Am. Chem. Soc. 117 (1995) 7291.
- [25] T.P. Gill, K.R. Mann, Organometallics 1 (1982) 485.